Computers & Structures Vol. 16, No. 1–4, pp. 89–98, 1983
Printed in Great Britain.

0045/7949/83/010089–10$03.00/0

OUR DISCRETE-KIRCHHOFF AND ISOPARAMETRIC SHELL ELEMENTS FOR NONLINEAR ANALYSIS—AN ASSESSMENT

KLAUS JÜRGEN BATHE and EDUARDO DVORKIN
Department of Mechanical Engineering, Massachusetts Institute of Technology, Cambridge, MA 02139, U.S.A.

and

LEE W. HO
ADINA Engineering, Inc., 71 Elton Avenue, Watertown, MA 02172, U.S.A.

Abstract—The theory and use of two effective shell elements are briefly surveyed, assessed and compared. The elements considered are our high-order (degenerate) isoparametric shell element and our simple flat triangular element, which both can be employed for analysis of large displacement/large rotation and plastic response of general shell structures. Specific emphasis is placed on the theoretical differences between the elements and some resulting practical consequences.

1. INTRODUCTION

During the recent years it has become apparent that two approaches for the development of general shell elements are very appropriate (see, e.g. [1, 2]):

—The use of relatively simple elements in which the bending and membrane actions, evaluated using plate theory and plane stress theory, are superimposed.

—The use of (degenerate) isoparametric elements in which fully three-dimensional stress and strain conditions are degenerated to shell behavior.

Various shell elements falling into each of the above categories have been developed, and it is apparent that there may be distinct advantages in using an element of one or the other category.

The objective in this paper is not to survey or discuss the many elements available but to only briefly survey, compare and assess two effective elements that we have developed for linear and nonlinear analysis, and that fall into the above approaches [3, 4]. The two elements are our simple discrete Kirchhoff theory and our high-order degenerate isoparametric elements. The starting point in the development of both these elements is, in essence, a plate/shell theory which includes shear deformations.

Although no doubt very effective for analysis of problems in which shear deformations contribute to the response of the shell structure, special considerations are necessary when the isoparametric element is employed for *very* thin shells. In this case the element must be able to satisfy the constraint of insignificant shear deformations. Our objective in this paper is to discuss the performance of the element in this regard.

An alternative, very elegant and effective approach towards satisfying the constraint of zero shear deformations is to use the discrete Kirchhoff theory. This approach can directly be employed to establish simple shell elements and our DKT (discrete Kirchhoff triangular) element is one of that kind [5–7].

Both elements can be employed for large displacement and elastic–plastic analysis, but there are distinct differences in the elastic–plastic descriptions used for the elements. In this paper we discuss these differences and provide some insight into the assumptions used and the practical consequences.

2. KINEMATICS OF THE SHELL ELEMENTS

The starting point of the formulations of both elements is the interpolation of bending and shear deformations. In the case of the isoparametric degenerate element we have for an element with q mid-surface nodes the displacements at time t

$$ {}^{t}u_i = \sum_{k=1}^{q} h_k \, {}^{t}u_i^k + \frac{t}{2} \sum_{k=1}^{q} a_k h_k ({}^{t}V_{ni}^k - {}^{0}V_{ni}^k) \qquad (1) $$

where the ${}^{t}u_i$ are the displacements (of a material point of the element) measured in the stationary Cartesian coordinate axes ${}^{0}x_i$, ${}^{t}x_i$, the h_k are the isoparametric interpolation functions, the ${}^{t}u_i^k$ are the nodal point displacements at node k, a_k is the thickness of the element at node k, and the ${}^{t}V_{ni}^k$ and ${}^{0}V_{ni}^k$ are the direction cosines of the mid-surface "normal" vector at nodal point k at times t and 0, respectively. The relation in eqn (1) is obtained from the interpolation of the element coordinates at times 0 and t. Similarly, the incremental displacements u_i from the configuration at time t are,

$$ u_i = \sum_{k=1}^{q} h_k \, u_i^k + \frac{t}{2} \sum_{k=1}^{q} a_k h_k (-{}^{t}V_{2i}^k \alpha_k + {}^{t}V_{1i}^k \beta_k) \qquad (2) $$

where the ${}^{t}V_{2i}^k$ and ${}^{t}V_{1i}^k$ are the direction cosines of the two nodal point vectors that are normal to each other and that are normal to ${}^{t}\mathbf{V}_n$, and α_k and β_k are the rotations about these vectors (see Fig. 1). Using eqns (1) and (2) the shell element matrices for a total Lagrangian and an updated Lagrangian formulation have been presented in Refs. [2, 3]. It may be noted that the element is subject to and can be employed in the following analysis conditions:

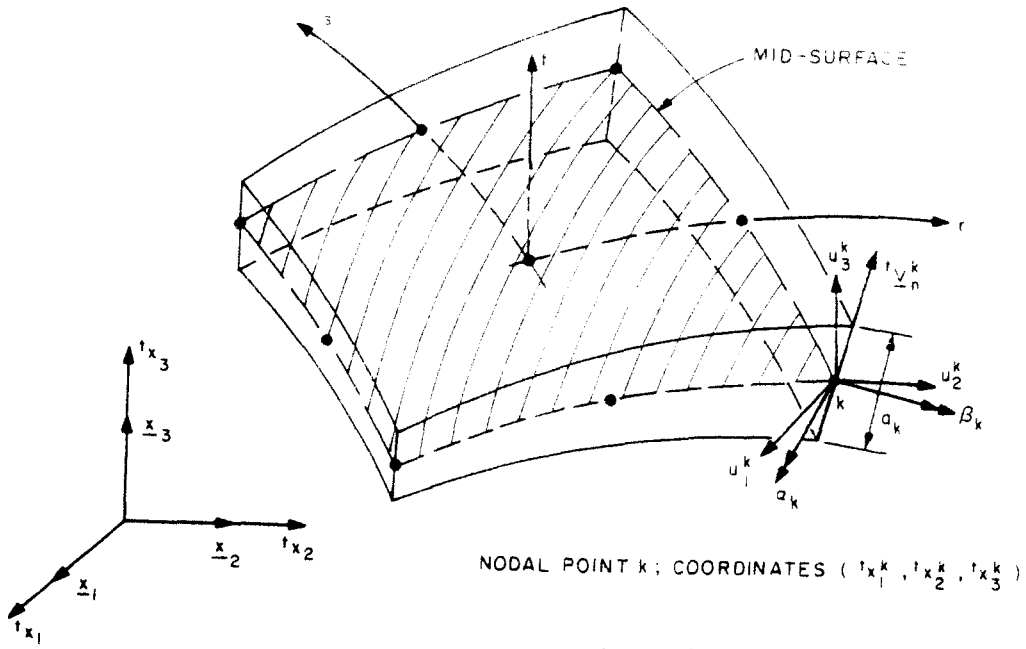

Fig. 1. Isoparametric (degenerate) nine-node shell element.

—Arbitrary large displacements/large rotations, but small strains

Here it should be noted that we are updating the nodal point coordinates and the nodal point normal vectors in a completely consistent manner for very large displacements and rotations. However, since the thickness of the element (a_k = thickness at nodal point k) is not updated during the solution, the element is only applicable to small strain analysis. With this restriction, the T.L. formulation is particularly attractive. Namely, since the components of the second Piola–Kirchhoff stress and Green–Lagrange strain tensors are invariant under rigid body motions, the stress–strain (elastic–plastic) relations can directly be integrated without updating for element fibre rotations.

—Five degrees of freedom per node

Having specified the coordinates and the normal vector ${}^0\mathbf{V}_n^k$ at each shell node, two incremental rotations at each of the nodal points are calculated that are used to update the directions of the normal vectors. This is a *very natural and general approach* to describe the kinematics of shell behavior. The approach can also directly be extended to formulate shell-to-solid transition elements ([2], p. 250).

—Thick and thin shells

The element is formulated including shear effects (as in the Mindlin plate theory), although these are included assuming a constant shear stress over the element thickness. Hence, the element is directly applicable to the analysis of moderately thick shells. However, when the element is used for thin shell analysis it is important that the constraint of zero (or very small) shear strains can be satisfied. This necessitates care in selecting the appropriate element (geometry and displacement) interpolation functions. We discuss our detailed thoughts on this matter in Section 4.

The displacement interpolation used in eqn (2) is also the basic equation employed in the formulation of our discrete Kirchhoff flat triangular element. However, now this interpolation is used with respect to the *current* geometry of the element and the bending and membrane displacements are interpolated to different order, see Fig. 2. To render the element applicable to very thin shells, the shearing strain contribution is simply neglected and the section rotations are tied to the transverse displacements of the element using the Kirchhoff hypothesis of zero shear strains. The updated Lagrangian formulation is based on updating the stress-state and the geometry of the element in the incremental solution. This DKT element is subject to and can be employed in the following analysis conditions:

—Arbitrary large displacements and rotations, but small strains

The restriction of small strains follows because the thickness and surface area of the element are not updated during the solution.

—Six degrees of freedom per node

The motion of the element is described using the six engineering degrees of freedom at each node (3 translations and 3 rotations corresponding to the stationary Cartesian coordinate system). This results in a relatively easy use of the element for modeling shell structures.

—Thin shells

Since the shear strain energy is neglected and the Kirchhoff hypothesis is imposed, the element is only applicable to the analysis of thin (including *very* thin) shells.

We may note here that we regard the approach used to develop this thin shell element from the Mindlin plate theory as a most natural, theoretically sound and effective procedure. It does not require the determination and use of "numerical factors to make the element work", totally avoids the problem of element locking (see Section 4) and preserves the full rank of the element stiffness matrix.

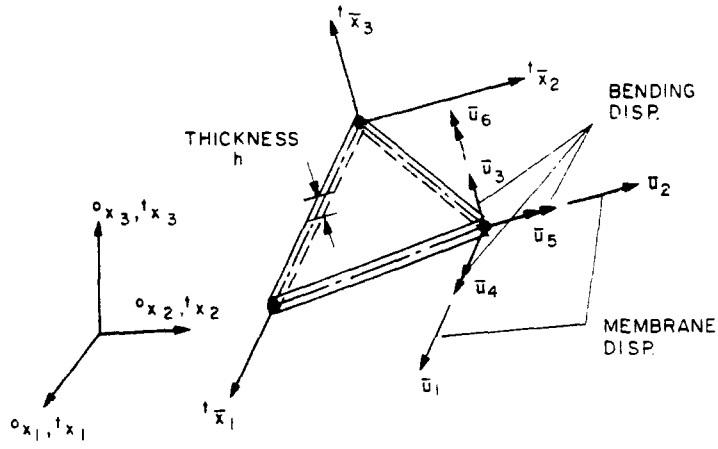

(a) Element with Local and Global Coordinate Systems

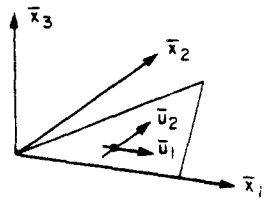

Linear variation of disp. $\bar{u}_1$, $\bar{u}_2$ within element

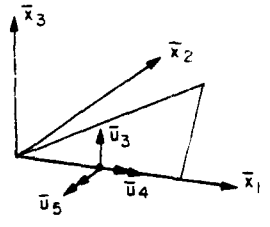

Cubic variation of transverse disp. $\bar{u}_3$, quadratic variation of rotation $\bar{u}_5$ and linear variation of rotation $\bar{u}_4$ along each side of element

Fig. 2. Three-node DKT plate/shell element.

—*Use of fine meshes*

Since the element is flat and the coupling between the membrane and bending actions is only introduced by the transformations of the nodal point degrees of freedom from the local to the global coordinate directions, it is necessary to use a relatively large number of elements in the discretization of a general shell structure. This, however, is offset by the small cost per element.

The kinematic formulations of the elements have been described in detail earlier in Refs. [2–5], and we therefore discuss in the following sections the formulations for elastic–plastic analysis, and give some insight into the application of the isoparametric element to very thin shells.

3. ELASTIC-PLASTIC FORMULATIONS

In accordance with the level of approximations used in the kinematic formulations of the elements we use for the isoparametric element an accurate elastic–plastic description and for the DKT element a more approximate evaluation. Namely, for the isoparametric element we operate with the shell element stresses on the fundamental elastic–plastic relations of flow theory whereas for the DKT element we use an interaction diagram of section moments and membrane forces. In each case we use the basic procedure summarized in Table 6.12 of Ref. [2].

3.1 *Isoparametric element*

For the isoparametric element we transform the Cartesian total strain components to correspond to mid-surface coordinate directions, and we then update the stresses in those directions. These calculations contain the assumption of zero stress normal to the shell mid-surface. The complete solution process can be summarized as follows:

—At each integration point calculate the incremental total strains corresponding to shell mid-surface coordinate directions. We simply use the t-direction as the normal direction to the shell mid-surface. This can be an approximation, but the direction cosines are easily obtained from the Jacobian operator $\mathbf{J}$, which anyway must be calculated for the evaluation of the strain–displacement matrix. The other mid-surface coordinate directions $\bar{r}$, $\bar{s}$ are obtained as shown in Fig. 3. Note that these coordinate directions are directly obtained by the calculations in Fig. 3 using the columns in $\mathbf{J}$.

—Integrate over the incremental total strains to obtain the total new stress components corresponding to the $\bar{r}$, $\bar{s}$, t coordinate directions. The stress–strain matrix is evaluated as in fully three-dimensional analysis but using

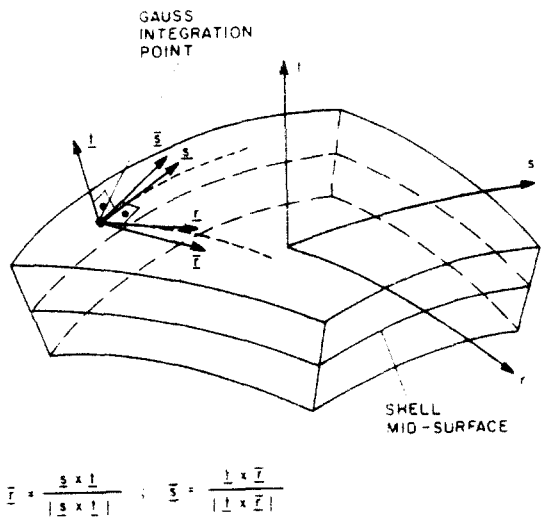

Fig. 3. Construction of orthogonal system of coordinate axes ($\bar{r}$, $\bar{s}$, $\bar{t}$) for strain and stress calculation at an integration point.

the condition that the Cauchy stress normal to the shell mid-surface vanishes. In this integration, we evaluate also the total plastic strains at the integration point.

—For the evaluation of the stiffness matrix and the calculation of the element force vector, the calculated shell mid-surface aligned element stresses and the corresponding material stress–strain law are transformed to the global Cartesian coordinate axes. The stiffness matrix and element force vector are then calculated as described in Table 6.8 of Ref. [2].

—In a large displacement analysis the same solution process is employed but 2nd Piola–Kirchhoff stresses and Green-Langrange strains are used instead of the stress and strain measures of infinitesimal displacement analysis.

The above calculation of stresses and strains is carried out at each integration point of the element, and the integration is performed over the element thickness and mid-surface. Hence, the spread of plasticity through the element thickness and over the element is modeled, and high solution accuracy can be expected. However, a disadvantage of the analysis is its relatively high solution cost.

3.2 *Discrete Kirchhoff triangular element*

The premise of the DKT element is the small cost per element, but as pointed out earlier, a relatively large number of elements must be used to model a complex shell behavior. Hence, it is natural to employ also a plasticity description that keeps the calculation cost of the element matrices at a low level.

Since the element matrices have been formulated using stress resultants, our objective is to establish at the integration points of the mid-surface the elastic–plastic stress–strain matrices that correspond to the current states of section forces and moments. These matrices could be evaluated using the plasticity matrices of plane stress analysis and integrating these through the thickness of the element—in the same way as the elastic properties for bending moments and membrane forces are calculated.

However, in accordance with the overall objective to obtain a cost-effective element, we decided to rather employ stress resultants in the description of the plastic behavior, so that no numerical integration through the element thickness is carried out. Following the developments advanced by Ilyushin and Robinson[8, 9], an appropriate yield function for thin shells is, for the stress conditions at time t,

$$ {}^{t}f = {}^{t}\bar{Q}_M + {}^{t}\bar{Q}_B + {}^{t}\bar{Q}_{MB} - \gamma({}^{t}\sigma_0)^2 = 0 \tag{3} $$

where

$$ {}^{t}\bar{Q}_M = \frac{1}{h^2}\{({}^{t}\bar{N}_1)^2 + ({}^{t}\bar{N}_2)^2 - {}^{t}\bar{N}_1\,{}^{t}\bar{N}_2 + 3({}^{t}\bar{N}_{12})^2\} $$

$$ {}^{t}\bar{Q}_B = \frac{16}{h^4}\{({}^{t}\bar{M}_1)^2 + ({}^{t}\bar{M}_2)^2 - {}^{t}\bar{M}_1\,{}^{t}\bar{M}_2 + 3({}^{t}\bar{M}_{12})^2\} \tag{4} $$

$$ {}^{t}\bar{Q}_{MB} = \frac{12}{h^3}\left\{\left(\frac{1}{3}({}^{t}\bar{N}_1\,{}^{t}\bar{M}_1 + {}^{t}\bar{N}_2\,{}^{t}\bar{M}_2) + {}^{t}\bar{N}_{12}\,{}^{t}\bar{M}_{12} - \frac{1}{6}\right.\right. $$
$$ \left.\left. \times ({}^{t}\bar{N}_1\,{}^{t}\bar{M}_2 + {}^{t}\bar{N}_2\,{}^{t}\bar{M}_1)\right)\right\} \tag{5} $$

and ${}^{t}\bar{N}_1$, ${}^{t}\bar{N}_2$, ${}^{t}\bar{N}_{12}$ are the section membrane forces, ${}^{t}\bar{M}_1$, ${}^{t}\bar{M}_2$, ${}^{t}\bar{M}_{12}$ are the section moments and ${}^{t}\sigma_0$ is the current yield stress obtained from a simple tension test; γ is a constant with a recommended value of $(1/\sqrt{3})$ in Ref. [9]. Figure 4 depicts this yield function.

In order to obtain a relation for the plastic strain increments, $\bar{\mathbf{e}}^P$, and the plastic curvature increments, $\bar{\boldsymbol{\kappa}}^P$, the normality rule is employed stating that the flow direction is always normal to the yield surface. Hence,

$$ \bar{\mathbf{e}}^P = \lambda\,{}^{t}\bar{\mathbf{f}}_M \tag{6} $$

$$ \bar{\boldsymbol{\kappa}}^P = \lambda\,{}^{t}\bar{\mathbf{f}}_B \tag{7} $$

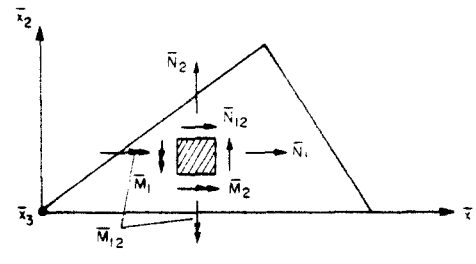

(a) Element Section Forces and Moments

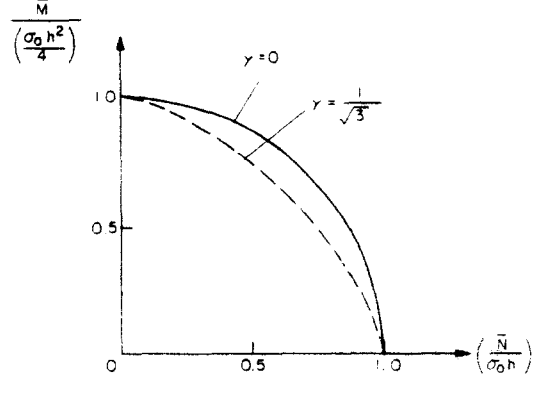

(b) Uniaxial Yield Condition

Fig. 4. Yield condition used with the DKT element.

where

$$ {}^{t}\bar{\mathbf{f}}_M{}^T = [\partial {}^{t}f/\partial {}^{t}\bar{N}_1 \;\; \partial {}^{t}f/\partial {}^{t}\bar{N}_2 \;\; \partial {}^{t}f/\partial {}^{t}\bar{N}_{12}] $$
$$ {}^{t}\bar{\mathbf{f}}_B{}^T = [\partial {}^{t}f/\partial {}^{t}\bar{M}_1 \;\; \partial {}^{t}f/\partial {}^{t}\bar{M}_2 \;\; \partial {}^{t}f/\partial {}^{t}\bar{M}_{12}] \tag{8} $$

and λ is a parameter to be determined such that the products of the stress-resultants and their corresponding plastic strain increments are equal to the plastic work increment (per unit area)

$$ d{}^{t}W^p = {}^{t}\bar{\mathbf{N}}^T \bar{\mathbf{e}}^p + {}^{t}\bar{\mathbf{M}}^T \bar{\boldsymbol{\kappa}}^p. \tag{9} $$

In our work we have so far only considered isotropic hardening materials. The adopted hypothesis in the hardening rule is that the yield stress at any loading stage (${}^{t}\sigma_0$) is a function of the plastic work per unit area. An explicit relation can be obtained by performing a simple tension test in which the elastic and hardening moduli of the material are denoted by E and E_T, respectively.

$$ {}^{t}W^p = \frac{h}{2}\left(\frac{1}{E_T} - \frac{1}{E}\right)({}^{t}\sigma_0{}^2 - {}^{0}\sigma_0{}^2) \tag{10} $$

where ${}^{0}\sigma_0$ is the initial yield stress. The rate of change of the current yield stress with respect to the plastic work per unit area is given by

$$ \frac{d{}^{t}\sigma_0}{d{}^{t}W^p} = \frac{H}{{}^{t}\sigma_0}; \quad H = \frac{E\,E_T}{h(E - E_T)}. \tag{11} $$

Using next the plastic flow relation $d{}^{t}f = 0$ we obtain

$$ \lambda = \frac{1}{m + b + r}({}^{t}\bar{\mathbf{f}}_M{}^T \mathbf{C}^E \bar{\mathbf{e}} + {}^{t}\bar{\mathbf{f}}_B{}^T \mathbf{D}^E \bar{\boldsymbol{\kappa}}) \tag{12} $$

where

$$ m = {}^{t}\bar{\mathbf{f}}_M{}^T \mathbf{C}^E {}^{t}\bar{\mathbf{f}}_M; \quad b = {}^{t}\bar{\mathbf{f}}_B{}^T \mathbf{D}^E {}^{t}\bar{\mathbf{f}}_B $$
$$ r = 2H({}^{t}\bar{\mathbf{N}}^T {}^{t}\bar{\mathbf{f}}_M + {}^{t}\bar{\mathbf{M}}^T {}^{t}\bar{\mathbf{f}}_B) \tag{13} $$

and $\bar{\mathbf{e}}$ and $\bar{\boldsymbol{\kappa}}$ are the total (elastic plus plastic) strain and curvature increments. Substituting the value of λ into eqns (6) and (7) the incremental stress–strain relations become

$$ \bar{\mathbf{N}} = \mathbf{C}_M^{EP} \bar{\mathbf{e}} + \mathbf{C}_{MB}^{EP} \bar{\boldsymbol{\kappa}} \tag{14} $$

$$ \bar{\mathbf{M}} = (\mathbf{C}_{MB}^{EP})^T \bar{\mathbf{e}} + \mathbf{D}_B^{EP} \bar{\boldsymbol{\kappa}} \tag{15} $$

where

$$ \mathbf{C}_M^{EP} = \mathbf{C}^E - \frac{1}{m + b + r}\mathbf{C}^E {}^{t}\bar{\mathbf{f}}_M {}^{t}\bar{\mathbf{f}}_M{}^T \mathbf{C}^E \tag{16} $$

$$ \mathbf{C}_{MB}^{EP} = \frac{-1}{m + b + r}\mathbf{C}^E {}^{t}\bar{\mathbf{f}}_M {}^{t}\bar{\mathbf{f}}_B{}^T \mathbf{D}^E \tag{17} $$

and

$$ \mathbf{D}_B^{EP} = \mathbf{D}^E - \frac{1}{m + b + r}\mathbf{D}^E {}^{t}\bar{\mathbf{f}}_B {}^{t}\bar{\mathbf{f}}_B{}^T \mathbf{D}^E \tag{18} $$

in which $\mathbf{C}^E$ and $\mathbf{D}^E$ are the (generalized) elastic stress–strain relations. Note that when the material becomes plastic, the membrane and the bending resultants are coupled even though the geometry of the element remains flat.

The use of this plasticity description is illustrated in Section 5.

4. CHOICE OF ELEMENTS AND NUMERICAL INTEGRATION

Considering the discrete Kirchhoff theory element, we only have used the flat triangular element but the same concept has also been employed to develop a quadrilateral element[6] for linear analysis. There is relatively little choice in the numerical integration; i.e. 3 point integration should be used in elastic analysis to fully integrate the triangular element stiffness matrix. Since (for a linear elastic material) the element can only represent, in any orientation, a constant bending moment and a constant membrane force exactly, a higher integration order is also hardly justified for elastic–plastic analysis.

However, considering the isoparametric sheli element, the appropriate number of nodal points and the appropriate integration scheme and order must be chosen. For the discussion of these issues we distinguish between the analysis of moderately thick plates/shells and thin plates/shells.

Moderately thick plates and shells

These structures can be analyzed using the isoparametric element with any of its nodal configurations, but *the Lagrangian quadratic and cubic elements are usually most effective.* The integration schemes frequently best for these elements are 3×3 and 4×4 Gauss integration over the mid-surfaces but the uniform "reduced" integration 2×2 and 3×3 may be of advantage, when the elements are distorted (as discussed below). The order of Gauss integration through the element thickness depends on whether an elastic (2 point integration) or elastic–plastic (3 or 4 point integration) analysis is performed.

Thin plates and shells

The constraint to be satisfied in the analysis of very thin plates and shells is that of negligible transverse shear deformations. Hence, for a shell element to be applicable to the analysis of very thin plates and shells it is necessary that the element displacement interpolations can satisfy the constraint of zero transverse shear strains. Two different approaches can be used for this purpose. In the first approach an appropriate interpolation of displacements is used that admits the constraint of zero shear strains throughout the element[10], and in the second approach the original displacement functions do not admit zero shear strains everywhere in the element, but the stiffness matrix is not integrated exactly[11–13]. Therefore, the reduced or selective integration scheme employed to evaluate the stiffness matrix is such as to admit zero shear strains. This reduced integration can actually be identified as effectively *using* different strain interpolations than those chosen originally, and the total analysis procedure results in the use of a mixed method.

The problem with using reduced or selective integration for *general nonlinear complex shell analysis* is to ensure that [2]

(1) The element does not contain any spurious zero energy modes.

(2) The element is complete and passes the patch test.

The use of selective integration has been somewhat

successful for lower-order elements. However, as pointed out above, for low-order elements we believe that the discrete Kirchhoff approach is more effective. For the higher-order elements, the constraint of zero shear strain can be satisfied, as discussed in Ref. [10], provided the elements are undistorted. Namely, the important conclusion in Ref. [10] was that in practice the Lagrangian parabolic and cubic elements do not lock for any thickness to length ratios. However, this conclusion was only applicable to *undistorted* elements and must be revised when distorted elements are considered.

Based on the experiences discussed further in Section 5.3, we therefore note that the parabolic 9-node and 16-node Lagrangian elements should be employed and the following integration schemes are usually effective: *for flat and undistorted elements*, i.e. the Jacobian matrix **J** is a diagonal matrix with constant entries, 4×4 integration for the cubic element and 3×3 integration for the quadratic element; *for distorted elements* (**J** is non-diagonal and a function of the coordinates), 3×3 integration for the cubic element and 2×2 integration for the quadratic elements.

The recommendation to use the lower-order integration for the distorted elements is based on the fact that the *effective* interpolation of the element strains may be significantly lower than for the undistorted elements. This decrease in the order of strain interpolation is a result of the inverse of the Jacobian matrix used in the evaluation of the strain interpolation matrix. Hence, the formulation in [10] must now also involve the distortion of the elements and there seems to be no general way to extend this formula for direct and easy use. However, with uniform reduced integration the under-integrated element passes the patch test and element locking is frequently avoided. Furthermore, spurious kinematic modes may not be encountered because of the reduction in strain interpolation.

In the case of analysis of shells, the curvature of the shell "distorts" the element, and it depends on the "arc extended" by the element whether the lower-order integration is appropriate.

These observations lead to the following conclusions useful for actual practical shell analysis:

—The locking of an element is an *element property* and hence the element aspect ratio (length/thickness) and element distortion must be kept a minimum. If these conditions are met high-order integration (3×3 Gauss integration for the quadratic and 4×4 Gauss integration for the cubic element) provides a reliable solution.

—To establish an appropriate mesh for the analysis of a shell it may be useful to test a single element with the typical thickness and curvature of the shell. The analysis of the element (which should have typical dimensions to be used in the actual shell analysis) subjected to a

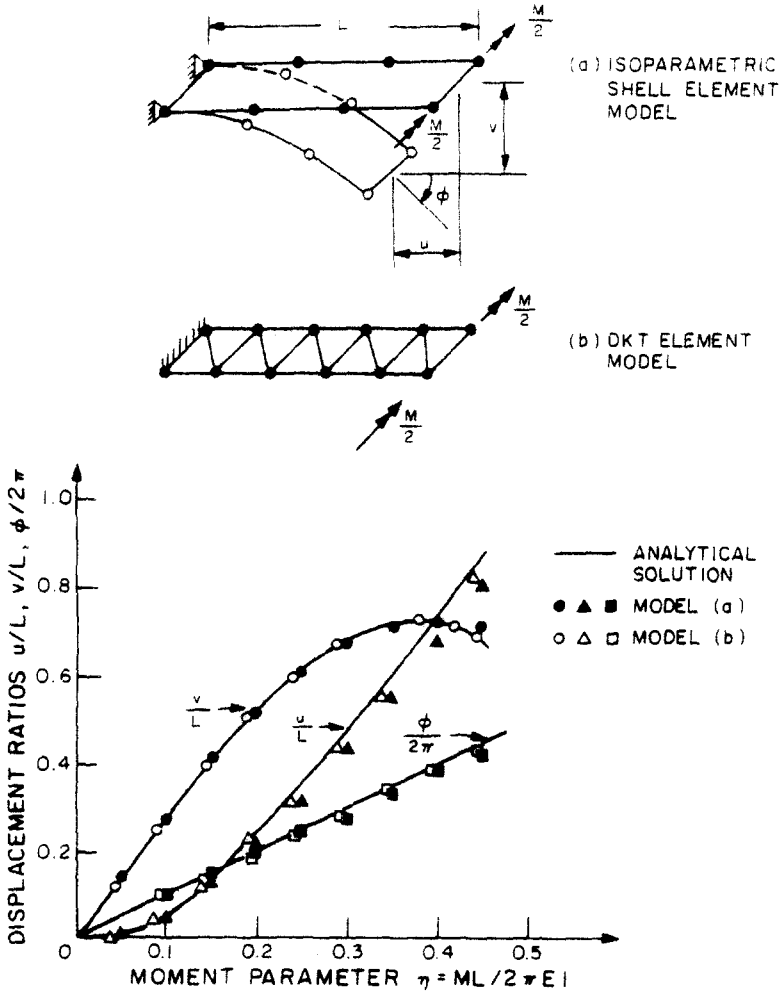

Fig. 5. Elastic cantilever; large displacement analysis.

bending moment would display whether the element is too large or reduced integration is appropriate.

5. SOME SIMPLE NUMERICAL EXPERIMENTS

The following problems provide some simple test cases that we have selected in our study to demonstrate some of the element features described in the preceding sections. Additional solutions using the elements can be found in Refs. [3–5, 7, 10, 14–16].

5.1 *Large displacement analysis of a cantilever*

Figure 5 shows the finite element model used for the analysis of the cantilever. One simple cubic isoparametric element and 5 layers of the DKT element have been employed. The same figure also shows the response predicted, and it is seen that both models are adequate for the large displacement prediction.

5.2 *Elastic–plastic large displacement analysis of a cantilever*

Figure 6 gives the model used in this elastic–plastic analysis. The response predicted for the structure shows the expected characteristics. Namely, the DKT element model reaches full plasticity through the cross-section at point A, after which more load can only be carried because of the strain hardening of the material, line A to B. On the other hand, for the shell model the plasticity has reached the outer integration points at point C, and then the inner integration points (measured from the shell mid-surface) at point D. Hence, using the isoparametric element, the effect of plasticity is modeled as the plasticity progresses through the thickness of the shell.

The effect of the integration order used on the prediction of the plastic collapse of a shell element in a simple stress state when compared to the Ilyushin theory is given in Fig. 7. Note that the discrepancy in the analysis results is very large when too low an order of integration is used [2].

5.3 *Some experiments on the use of the isoparametric shell element*

The objective with the experiments reported here was to investigate the behavior of the isoparametric parabolic and cubic Lagrangian elements when the elements are used in the analysis of shells and when they are distorted and integrated with high and low-order Gauss integration.

Figure 8 shows a simple 16-node element model used

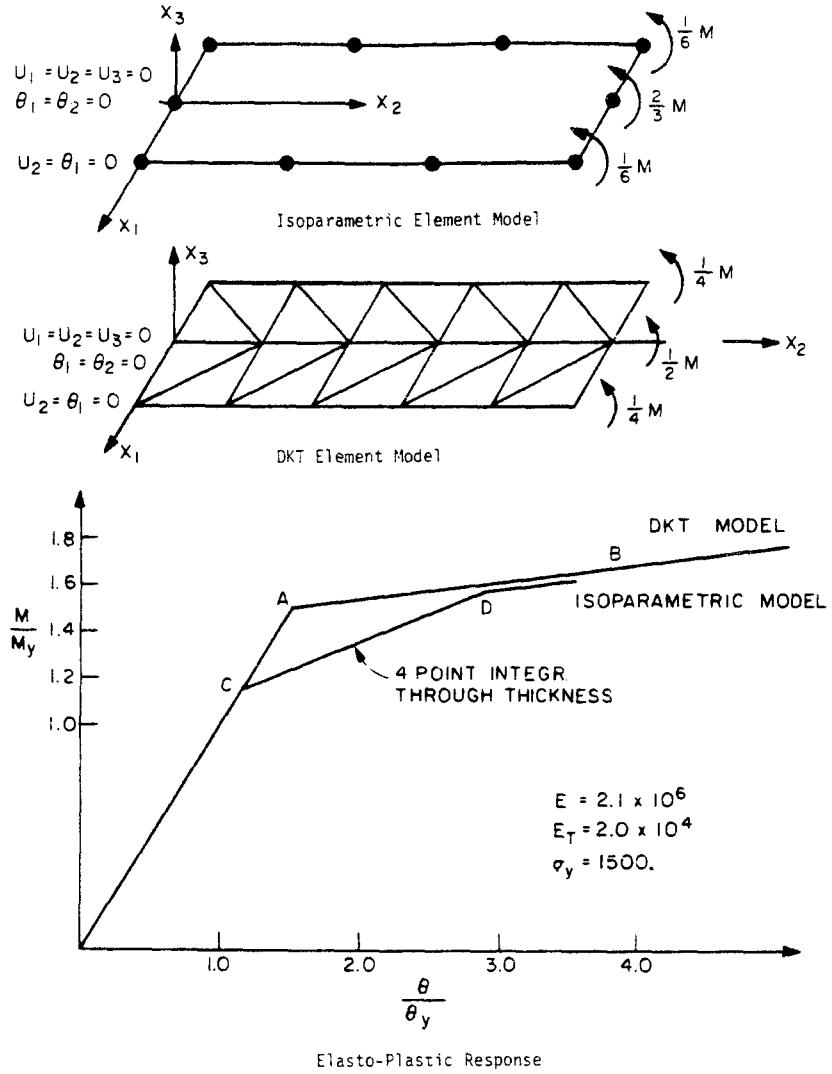

Fig. 6. Elasto–plastic analysis of cantilever.

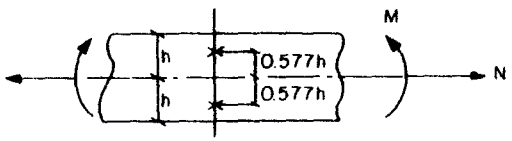

INTEGRATION WITH 2 POINTS ACROSS THICKNESS

STRESS-STATE CONSIDERED

N	$\frac{M_S}{M_I}$			
	∞ int. points	4 int. points	3 int. points	2 int. points
$N_y/3$	1.04	0.92	1.01	0.90
$2N_y/3$	0.95	0.99	0.89	0.66

$N_y = \sigma_y 2h$; M_S = collapse moment of shell element

M_I = collapse moment by Ilyushin theory

Fig. 7. Comparison of collapse loads.

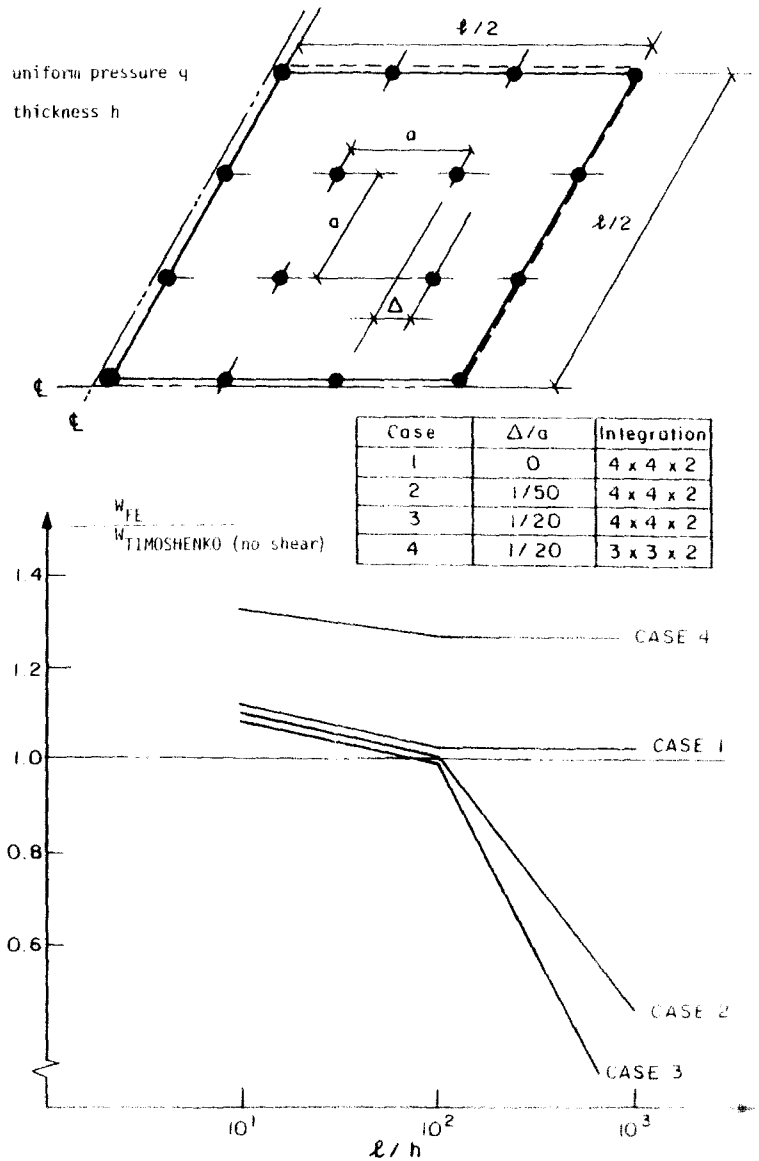

Case	Δ/a	Integration
1	0	4 x 4 x 2
2	1/50	4 x 4 x 2
3	1/20	4 x 4 x 2
4	1/20	3 x 3 x 2

Fig. 8. Analysis of simply-supported plate model.

for the analysis of a simply-supported square plate. The analyses conducted and results obtained are also summarized in the figure. We observe that the distorted element locks with 4×4 integration, but that reduced integration relieves the locking. Furthermore, for a ratio of *element* length to *element* thickness less than 100, the performance of the fully integrated element is excellent.

These observations also hold for a large displacement solution of the model using the total Lagrangian (or updated Lagrangian) formulation.

Figure 9 shows a curved cantilever modeled using one single parabolic element and the results obtained using a high integration order. We observe that for larger angles spanned by the element the results rapidly deteriorate. However, the locking phenomenon is an element property so that with 6 elements to model the 30 degree bend reasonable results are obtained. Figure 9 also shows that the cubic element behaves considerably better than the parabolic element, but this element behavior rapidly deteriorates when the element is distorted in its mid-surface.

Note that, as expected, the element behavior becomes less sensitive to distortion when the element thickness increases. For example, when one parabolic element is used to model the 30° bend at a thickness $h = 1.2$, the value for θ_{FE}/θ_{TH} is 0.46.

The use of reduced integration does not help in the solution of this model. Gauss integration of order 2×2 and 3×3 for the parabolic and cubic element models, respectively, results into spurious zero eigenvalues preventing the solution of the governing equations. This is different from the solution of the model used in the analysis of the simply-supported plate (see Fig. 8), for which reduced integration gives much improved results when the element is distorted.

Figure 10 illustrates the effect of distortions on an 8 node shell element. We observe that the in-plane element distortion does not reduce the number of spurious kinematic modes, whereas the out-of-plane distortion eliminates these modes.

6. CONCLUDING REMARKS

The analysis of complex shells requires the use of versatile, reliable and cost-effective finite elements, and an in-depth understanding of these modeling capabilities. The objective in this paper was to briefly summarize the theory and application of two finite elements. We considered in this paper only static analysis conditions but

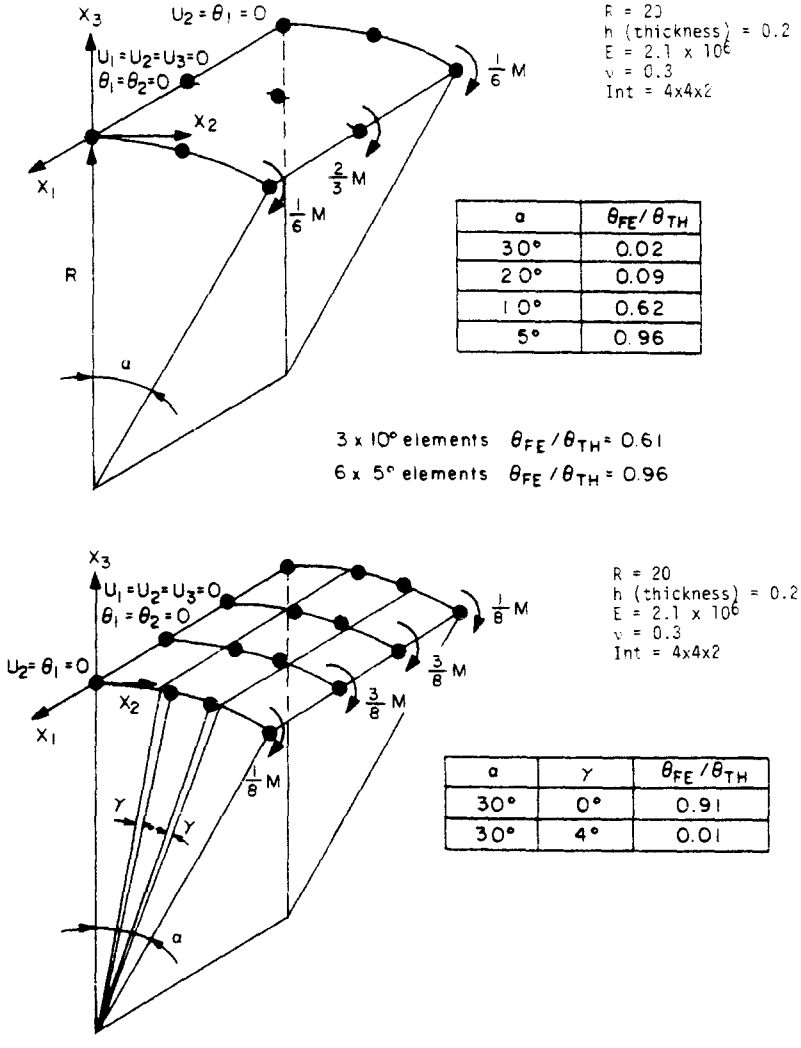

Fig. 9. Analysis of curved cantilever model. Note that the integration order for the parabolic element is higher than used in practice, and that at $\gamma = 4°$ the cubic element is highly distorted (not shown to scale).

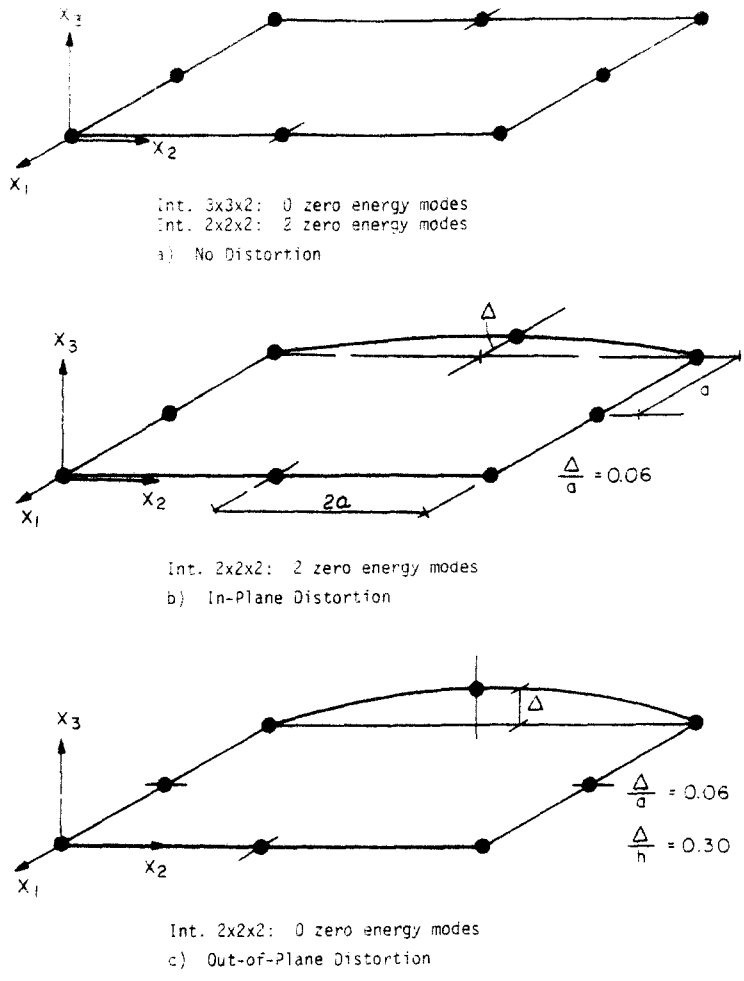

Fig. 10. Spurious zero energy modes in 8-node shell element.

the elements are also employed in dynamic response calculations.

The DKT and isoparametric elements represent the current state-of-the-art for nonlinear analysis, but further improvements are clearly very desirable. These improvements should primarily address the analysis of highly curved and thin shells in geometric and materially nonlinear analysis, and the analysis of large strain conditions.

Acknowledgement—We are grateful for the financial support of this work by the ADINA users group.

REFERENCES

1. O. C. Zienkiewicz, *The Finite Element Method.* McGraw-Hill, New York (1977).
2. K. J. Bathe, *Finite Element Procedures in Engineering Analysis.* Prentice-Hall, Englewood Cliffs, New Jersey (1982).
3. K. J. Bathe and S. Bolourchi, A geometric and material nonlinear plate and shell element. *Comput. Structures* **11**, 23–48 (1979).
4. K. J. Bathe and L. W. Ho, A simple and effective element for analysis of general shell structures. *Comput. Structures* **13**, 673–682 (1980).
5. J. L. Batoz, K. J. Bathe and L. W. Ho, A study of three-node triangular plate bending elements. *Int. J. Numer. Meth. Engng* **15**, 1771–1812 (1980).
6. J. L. Batoz and M. Ben Tahar, Evaluation of a new quadrilateral thin plate bending element. *Int. J. Numer. Meth. Engng* in press.
7. J. L. Batoz and G. Dhatt, An evaluation of two simple and effective triangular and quadrilateral plate bending elements. *Proc., New and Future Developments in Commercial Finite Element Methods*, pp. 352–368, Los Angeles, Oct. 1981.
8. A. A. Ilyushin, *Plasticite.* Eyrolles, Paris (1956).
9. M. Robinson, A comparison of yield surfaces for thin shells. *Int. J. Mech. Sci.* **13** (1971).
10. K. J. Bathe and L. W. Ho, Some results in the analysis of thin shell structures. *Nonlinear Finite Element Analysis in Structural Mechanics* (Edited by W. Wunderlich *et al.*), Springer-Verlag, Berlin (1981).
11. T. J. R. Hughes, R. L. Taylor and W. Kanoknukulchai, A simple and efficient finite element for plate bending. *Int. J. Numer. Meth. Engng* **11**, 1529–1543 (1977).
12. T. J. R. Hughes and W. K. Liu, Nonlinear finite element analysis of shells: part I, three-dimensional shells. *J. Comput. Meth. Appl. Mech. Engng* **26**, 331–362 (1981).
13. T. Belytschko and C. S. Tsay, A stabilization procedure for the quadrilateral plate element with one point quadrature. To be published.
14. ADINA—a finite element program for automatic dynamic incremental nonlinear analysis. Rep. AE 81-1, ADINA Engineering, Sept. 1981.
15. ADINA verification manual—problem solutions. Rep. AE 82-5, ADINA Engineering, October 1982.
16. K. J. Bathe (Ed), Nonlinear finite element analysis and ADINA. *Comput. Structures* **13**, 5/6 (1981).